International Journal on Advanced Science Engineering Information Technology

Vol.6 (2016) No. 5
ISSN: 2088-5334

Silica Sand Identification using ALOS PALSAR Full Polarimetry on The Northern Coastline of Rupat Island, Indonesia

Husnul Kausarian[#*], Josaphat Tetuko S Sumantyo[#], Hiroaki Kuze[#], Detri Karya[*], Good Fried Panggabean[#]

[#] *Center for Environmental Remote Sensing, Graduate School of Advance Integration Science, Chiba University, Chiba, 263-8522, Japan*
E-mail: kausarianhusnul@yahoo.com

** Engineering Geology, Faculty of Engineering, Universitas Islam Riau, Pekanbaru, 28284, Indonesia*
E-mail: husnulkausarian@eng.uir.ac.id

***Abstract*— Silica sand is one of the minerals which relatively abundant in Indonesia. One of the areas with abundant of silica sand distribution is the northern coastline of Rupat Island, Bengkalis district, Riau province, Indonesia. The distribution of silica sand in this island identified only on the northern coastline in this island. Some selected sample of silica sand was measured to get the percentage of silica sand mineral's content using X-Ray Fluorescence (XRF). Two adjacent scenes of ALOS PALSAR full-polarimetry were used. The physical properties of silica sand sample such as dielectric constant were measured using dielectric probe kit in the frequency range from 0.3 to 3.0 GHz and used for calculating the backscattering coefficient and the difference characteristics of silica sand with another object. Freeman-Durdeen and Yamaguchi techniques were used to get the scattering decomposition of physical scattering from the incoherent object model based. Surface scattering is the clearest of Scattering decomposition to show silica sand identification compares with other decompositions. From surface scattering, the backscattering coefficient value of silica sand was calculated starting from -59 dB until -52 dB. These values were given by the surface roughness condition, where the roughness is slightly rough planar. The flat condition supported by the grain size of silica sand particles that have almost the same size and shape, that were conducted by using microscopic photograph testing.**

***Keywords*— Silica Sand; ALOS PALSAR Full Polarimetry; Rupat Island; XRF**

I. INTRODUCTION

Silica sand is one of the minerals which relatively abundant in Indonesia [1], [2]. This is possible due to Indonesia geological condition, which has an almost acidic igneous rock that formed mineral's source. Silica sand can be found in the coastal area, rivers, lakes, beaches and some of the shallow seas. One of the areas which has been abundant with silica sand sedimentation is Rupat Island (Figure 1), Bengkalis district, Riau province, Indonesia. Silica sand in this island distributes in the north coastline area.

Space-borne remote sensing with its bird's view capability used for an alternative method for rapidly delineating and classifying surface sediments [3], [4], [5]. The optical/thermal and synthetic aperture radar (SAR) sensors are most useful for mapping and classifying the surface sediments. Usually, the reflected/emitted signals of backscattered SAR waves provide information about the physical properties of the objects. SAR data is very suitable to use for geological or geoscience study such as surface roughness and soil moisture estimations because the frequency or polarizations SAR measurements are carried out. The obtained multidimensional information allows the identification of different scatterers via discrimination of different scattering mechanisms [6]. The polarization information contained in the backscattered wave is directly related to the scatterer's geometrical structure, its orientation and even more important for geoscientific and related applications its geophysical properties [6], [7].

The purpose of this study is to identify and detection of silica sand distribution at the northern coastline of Rupat Island by analyzed the physical scattering technique using ALOS PALSAR data by calculated the relationship with the silica sand electrical characteristic properties and compare to the field data observation.

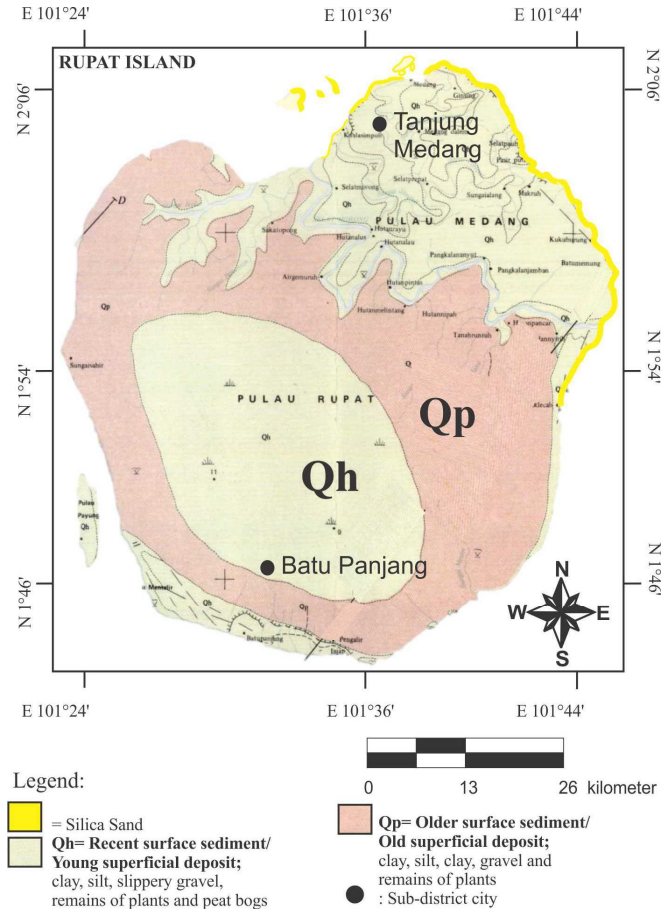

Fig. 1. Geological Map of Rupat Island.

II. Study Area

Rupat Island located at 1°41'12" N until 2°7'41" N and 101°23'19" E until 101°47'14" E with the total area about 1,500 km2. Rupat Island is divided into 2 subdistrict. Which is Rupat subdistrict with Batu Panjang as the capital and Rupat Utara subdistrict with Tanjung Medang as the capital.

Two main formations in Rupat Island are Recent Surface Sediment formation (Qh) and Older Surface Sediment formation (Qp). Old Superficial Deposit formation (Qp) consisting of clay, silt, clay, gravel and remains of plants. Young Superficial Deposit formation (Qh) consisting of clay, silt, gravel slippery, remains of plants and peat bogs. Those formations are recent age. Silica sand in this island comes from Malacca strait as the sediment transportation agent. Silica sand distributes only on the northern coastline of this island, for the southern coastline, it only has mud and small grain size of sand.

III. Materials and Method

A. Synthetic Aperture Radar

Two adjacent scenes of ALOS PALSAR full-polarimetry data (Table 1) were used, the full polarimetry ALOS PALSAR scene acquired on May 16, 2010, and on April 03, 2011. Analysis method and model of scattered waves from different types of topsoil (top layer) was developed [8]. This method introduced calculation of backscattering coefficient as the relation with the electrical properties of the object by using the impedance characters of the surface roughness.

Based on the ground measurements and to simplify the analysis, the impact of surface roughness on the scattered waves was not considered, where field measurements showed that the surface roughness was extremely shorter than the L-band wavelength (23.5 cm) [9], [10], [11]. In addition, the type of silica sand in this study area almost homogenous based on the chemical and physical laboratory analysis. Subsequently, the developed model was employed with the assumption that the layer composed of two layers: the first layer is silica sand and below silica sand layer is the peat layer as the bedrock.

The incident wave was assumed to be a plane wave with an incident angle θ_i. Where the effective impedance of silica sand layer, the parallel impedance of peat layer, and total input impedance are Z_S, Z_P, and Z_{TS}, respectively. To simplify the analysis, the parallel impedance of peat (Z_P) is neglected and assumed as zero (perfect conductor). From Fresnel's reflectivity coefficient and the total input impedance, the reflection coefficient can be described as:

$$\Gamma^0 = \left|\frac{1-\sqrt{\varepsilon_{rs}}}{1+\sqrt{\varepsilon_{rs}}}\right|^2 \quad (1)$$

Where ε_{rs} is the complex dielectric constant of silica sand, and the relationship between reflectivity coefficient with the reflection coefficient (Γ) is:

$$\Gamma = \Gamma^0 \cos\theta_i \quad (2)$$

Thus, the reflection coefficient can be described form the total input impedance (Z_{TS}) and the wave impedance in air or free space (Z_0), and described as:

$$\Gamma = \frac{Z_{TS} - Z_0 \cos\theta_i}{Z_{TS} + Z_0 \cos\theta_i} \quad (3)$$

Where Z_0 value is 120π ohms. Furthermore, the backscattering coefficient from field σ^0_f is defined as:

$$\sigma^0_f = 20\log(|\Gamma|) \quad (4)$$

ALOS PALSAR backscattering coefficient (σ^0_s) (dB) at a given polarization mode is:

$$\sigma^0_s = 10\log_{10}(DN) + CF \quad (5)$$

Where CF is the conversion factor (-83) [12].

From equation (4) and (5) we can get different value of backscattering coefficient from satellite and field observations. This differentiation called as average error and defined as:

$$\bar{e} = \overline{\sigma^0_s} - \overline{\sigma^0_f} \quad (6)$$

B. *Field Observation, Sample Validation and Laboratory Test*

TABLE I
SPECIFICATION OF ALOS PALSAR FULL-POLARIMETRY DATA OF RUPAT ISLAND

Configuration	Quadpol ALOS PALSAR Data	
	Scene 1	Scene 2
Acquisition date	05/16/2010	04/03/2011
Wavelength	23.5 cm	23.5 cm
Spatial resolution	1.27 GHz (L-Band) Az: 4.5 m Ra: 9.5 m	1.27 GHz (L-Band) Az: 4.5 m Ra: 9.5 m
Level product	P 1.1	P 1.1
Incidence angle at scene center	25.752	23.948
Orbit pass	Ascending	Ascending
Noise equivalent (NE σ^0)	-30 ~ -31 dB	-30 ~ -31 dB
Absolute geo-location accuracy	< 200 m	< 200 m
Absolute radiometric accuracy	0.7 dB	0.7 dB

This study covered the plotting of observation points for geological mapping, also sand sampling and testing in the laboratory. Field observation on the northern coastline of Rupat Island started with these areas: Tanjung Mumbul, Simpur Island, Kemunting Island, Babi Island, Beting Aceh, Pajak Island, Beruk Island, Tengah Island, Tanjung Medang, Teluk Rhu, Tanjung Punai, Tanjung Lapin, and Pasir Putih. Based on observation on the field, there are 16 observation locations with five main locations where samples collected in these areas. The areas are Tanjung Api (TAp), Teluk Rhu (TRh), Tanjung Punai (TPn), Tanjung Lapin (TLp) and Beting Aceh (BA). Silica sand sampling was conducted using the field sample collection such as excavation. The samples. All sample from the observation location shows the color of the sand is virtually white and homogeneous by direct observation in the field. It gave suggestion that the silica sand composition in this region have nearly the same silica content.

To determine the content of silica percentage and the compound of mineral properties, laboratory testing was used for the sand samples obtained from the field survey. The chemical analysis of silica sand samples is needed to get the types of compounds/elements, physical properties and percentage content of the compounds/elements.

A laboratory test was conducted to get the content of minerals in these samples. X-Ray Fluorescence (XRF) was used to get minerals content information. The microscopic photograph also used to know the shape and size of the fragment/grain of the minerals composition. From laboratory test using XRF (X-Ray Fluorescence), the result from silica sand samples shows the abundance of compounds such as SiO2, TiO2, Al2O3, Fe2O3, MnO, MgO, CaO, Na2O, K2O, and P2O5. XRF test was used to get compounds/minerals percentage content for 5 main locations (Tanjung Api, Teluk Rhu, Tanjung Punai and Tanjung Lapin).

IV. RESULT AND DISCUSSION

Two adjacent scenes of ALOS PALSAR full-polarimetry data were used for this study (see Table 1). From the equation (4) to (6) the differentiation value of backscattering coefficient between satellite and field observations have been calculated (Table 2). This differentiation is an error caused by the object orientation while measured from those.

TABLE II
BACKSCATTERING COEFFICIENT VALUE FROM ALOS PALSAR AND FIELD, AVERAGE ERROR AND AVERAGE RATIO

Location	Dielectric constant	Backscattering coefficient of field	Backscattering Coefficient of ALOS PALSAR
1	2.972	-53	-59
2	3.359	-49	-52
3	3.259	-50	-54
4	3.359	-49	-51
5	3.159	-51	-56
6	3.259	-50	-53
7	2.891	-56	-58
8	4.362	-42	-50
9	2.892	-54	-55
10	2.972	-53	-57
11	3.421	-48	-53
12	3.359	-49	-53
13	2.821	-55	-58
14	3.259	-50	-52
15	2.891	-56	-57
16	3.259	-50	-55
Average		-50.94	-54.56
The total average error (σ) is: (-54.56) – (-50.94) = -3.62			

The error of object measurement using field observation and satellite methods caused by surface roughness, multiple scattering, multiple objects at the same area (which mean has multiple dielectric constant), water content, humidity, weather condition, differentiation of incidence angle between field and satellite image measurement. From these conditions, the average error can be defined after measuring the samples taken from the field. Based on the sample properties measurement, dielectric constant shown an important factor influenced the value of backscattering coefficient compares with the other factors.

Freeman-Durdeen [13], [14] and Yamaguchi [15], [16], [17] (Figure 2) techniques were used to get the scattering decomposition of physical scattering from the incoherent object model based. These techniques are based on physical scattering where Freeman-Durdeen used 3 physical scattering types: Double bounce scattering, Surface scattering, and Volume scattering while Yamaguchi technique used four physical scattering types: Double bounce scattering, Surface scattering, Volume scattering and Helix scattering. These techniques were used to show the image of Rupat Island by using two adjacent images. In this study area, double bounce scattering represents in red to pink color, surface scattering represents in blue color, volume scattering represents in green color and helix scattering represents in yellow color. Silica sand distribution has dark color in their representation. This dark color given by the

surface roughness of silica sand distribution is almost flat (Figure 3).

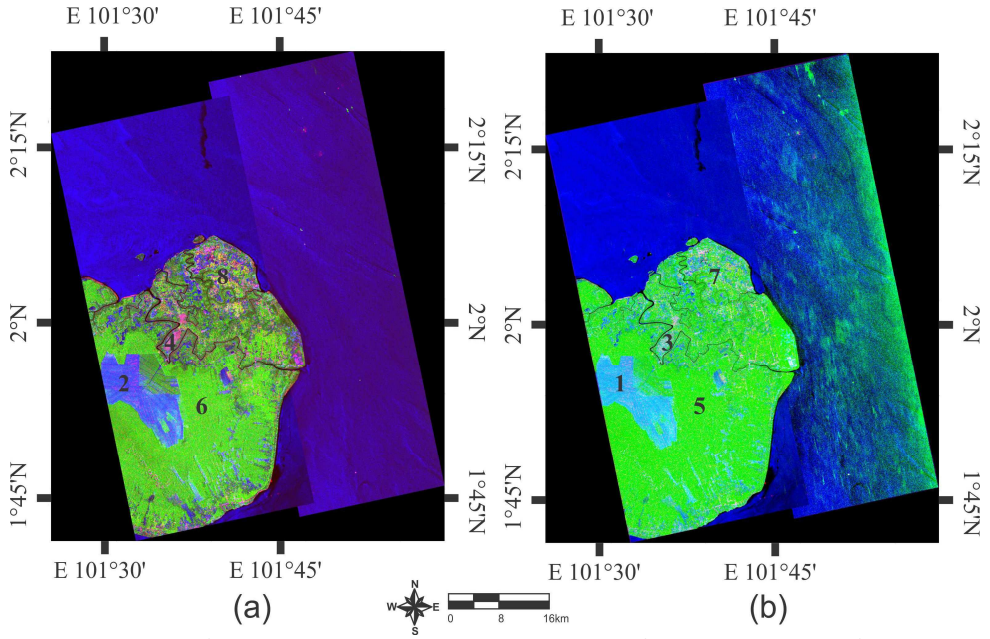

Fig. 2. Yamaguchi (Left) and Freeman-Durdeen Decomposition (Right) of Two Adjacent Scenes of Rupat Island.

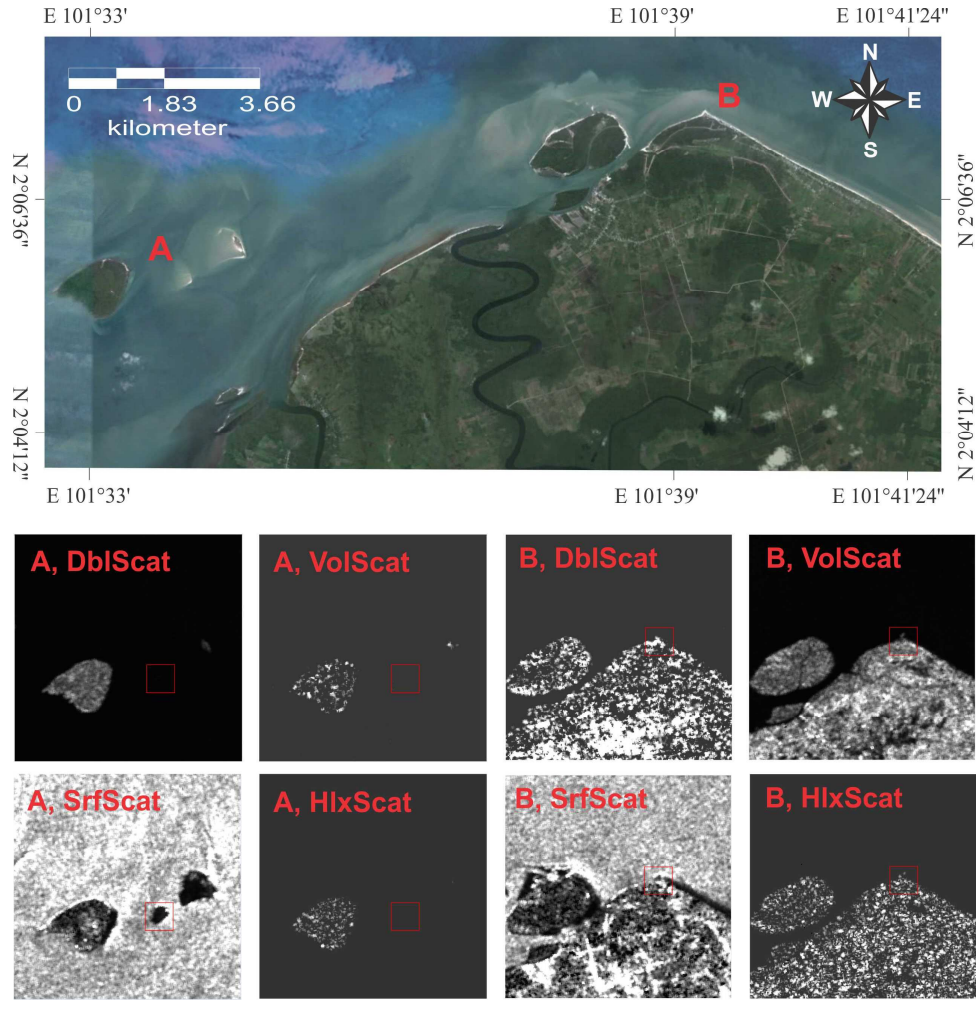

Fig. 3. Above: Google Earth's Image of Study Area, Below: Scattering decomposition image (A: Beting Aceh, B: Tanjung Api-Tanjung Punai).

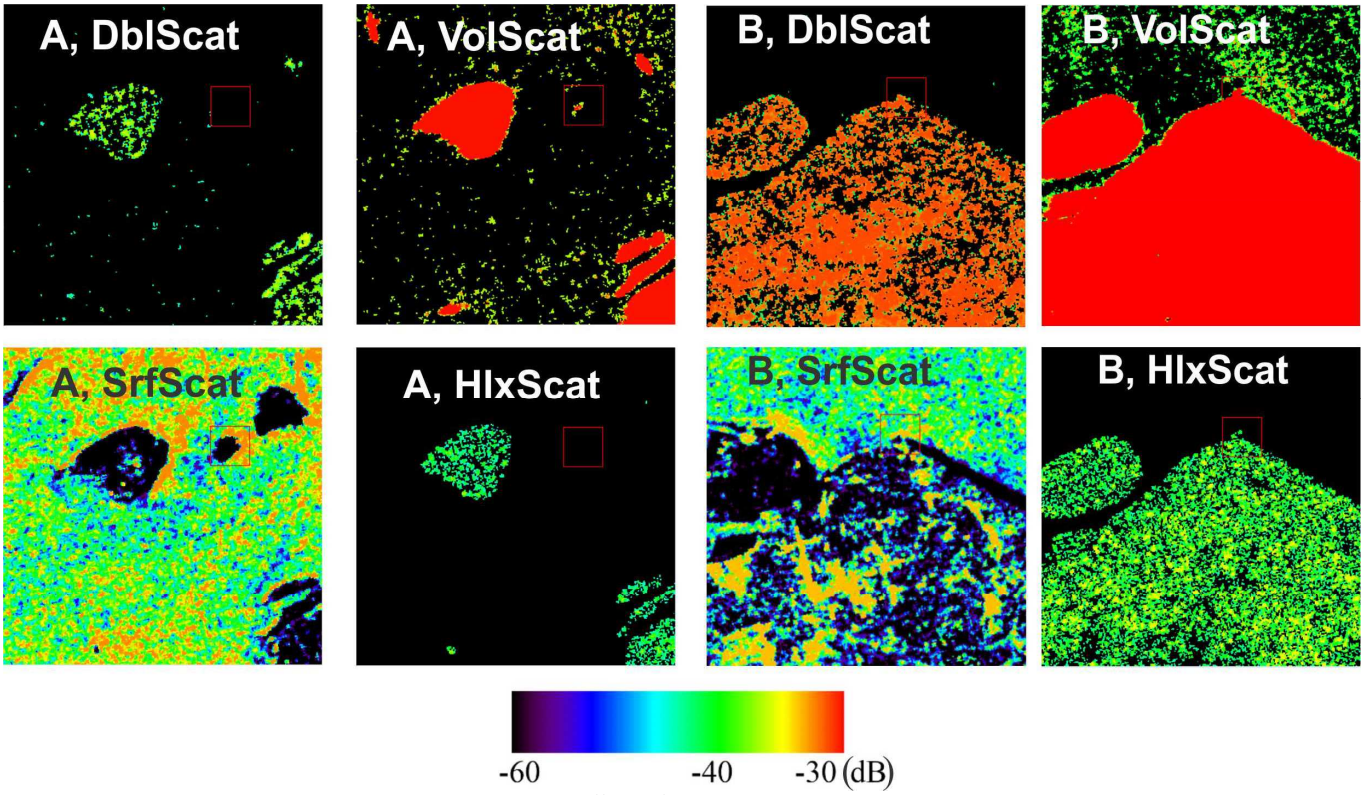

Fig. 4. Backscattering Coefficient from Each Polarimetric Decomposition.

From surface scattering, backscattering coefficient values of silica sand were calculated starting from -59 dB until -52 dB. These given by the roughness of silica sand surface is slightly rough planar, this condition supported by the grain size of silica sand particles that have nearly identical size and shape, that were conducted by using microscopic photograph testing. Microscopic photograph of silica sand sample (Figure 5) shows the shape and grain size of silica sand is nearly identical. Based on the sedimentation process by the transportation agent [18], [19], [20] it also suggests that silica sand in this study area was transported a far from its source. This analysis answered why silica sand appears only on the northern coastline because the silica sand came from non-in-situ, it was brought by the Malacca strait as the sediment transportation agent.

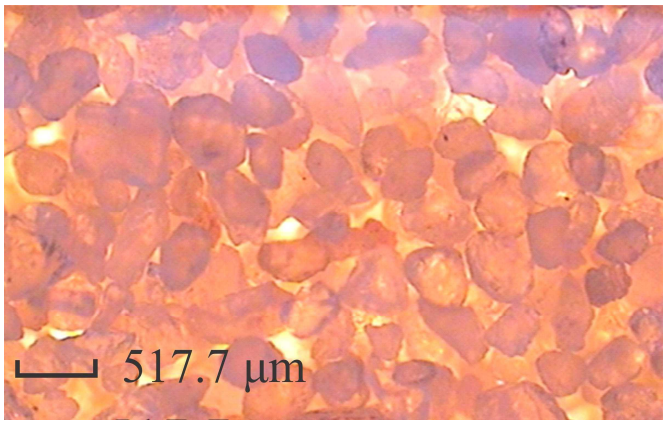

Fig. 5. Microscopic Photograph Shows the shape and grain size of Silica Sand Sample is almost same.

V. Conclusions

This research that was conducted on the northern coastline of Rupat Island shows the distribution of silica sand in this area. Silica sand characteristic in this area were studied using ALOS PALSAR full polarimetry data for its electromagnetic character. Silica sand in this study area gives the value of backscattering coefficient from -59 until -52 in dB value. This condition is given by surface scattering. For this area, the distribution of silica sand is almost flat. X-Ray Fluorescence (XRF) was supported the data analysis to prove the chemical properties value. By the XRF result, Silica content in this silica sand has the highest percentage compare than other minerals. The percentage of silica in the sample of silica sand from this study area is above 95%.

Acknowledgment

The authors would like to thank Lembaga Pengelola Dana Pendidikan (LPDP) for funding this research, government of Riau Province to provide research location, and Engineering Geology of Universitas Islam Riau. We also thank to the EORC JAXA ALOS PALSAR (Project #1024) and Josaphat Microwave Remote Sensing Laboratory (JMRSL) at CEReS, Chiba University who provides laboratory to measure the samples, Japanese Governement National Budget No. 2101, and Venture Business Laboratory (VBL) Chiba University.

REFERENCES

[1] N. Wicaksono, "Survei Potensi Pasir Kuarsa di Daerah Ketapang Propinsi Kalimantan Barat," *Jurnal Sains dan Teknologi Indonesia*, Vol. 11, June 2012.

[2] S. Purnawan, S. Karina, "Karakteristik dan kandungan mineral pasir pantai Lhok Mee, Beureunut dan Leungah, Kabupaten Aceh Besar," DEPIK, Vol. 3(3), Feb. 2015.

[3] D. M Kennedy, J. Milkins, "The formation of beaches on shore platforms in microtidal environments," Earth Surface Processes and Landforms, Vol. 40(1), pp. 34-46, Jan. 2015.

[4] E. Gallagher, H. Wadman, J. McNinch, A. Reniers, M.A. Koktas, "Conceptual Model for Spatial Grain Size Variability on the Surface of and within Beaches," Journal of Marine Science and Engineering, Vol. 4(2), pp. 38, May 2016.

[5] J. A Warrick, J. A. Bountry, A. E East, C. S. Magirl, T. J. Randle, G. Gelfenbaum, A. C Ritchie, G. R. Pess, V. Leung, J. J. Duda, "Large-scale dam removal on the Elwha River, Washington, USA: source-to-sink sediment budget and synthesis," Geomorphology, Vol. 246, p.p 729-50, Oct. 2015.

[6] J. S. Lee, L. A. Thomas, "The effect of orientation angle compensation on coherency matrix and polarimetric target decompositions," IEEE Transactions on Geoscience and Remote Sensing, Vol. 49, pp. 53-64, Jan. 2011.

[7] T. Jagdhuber, I. Hajnsek, K. P. Papathanassiou, "An iterative generalized hybrid decomposition for soil moisture retrieval under vegetation cover using fully polarimetric SAR," IEEE Journal of Selected Topics in Applied Earth Observations and Remote Sensing, Vol. 8(8), p.p 3911-22, Aug. 2015.

[8] P. Mishra, G. Shivangi and S. Dharmendra. "An impedance based approach to determine soil moisture using radarsat-2 data" In 2013 IEEE International Geoscience and Remote Sensing Symposium-IGARSS, pp. 2724-2727.

[9] D. Kachelriess, M. Wegmann, M. Gollock, N. Pettorelli, "The application of remote sensing for marine protected area management," Ecological Indicators, Vol 36, pp. 169-77. Jan. 2014.

[10] X. Monteys, P. Harris, S. Caloca, C. Cahalane, "Spatial Prediction of Coastal Bathymetry Based on Multispectral Satellite Imagery and Multibeam Data," Remote Sensing, Vol. 7(10), pp.13782-13806, Oct. 2015.

[11] Y. Tian, C. D. Peters-Lidard, K. W. Harrison, C. Prigent, H. Norouzi, F. Aires, S. A. Boukabara, F. A. Furuzawa and H. Masunaga, "Quantifying uncertainties in land-surface microwave emissivity retrievals," IEEE Transactions on Geoscience and Remote Sensing, 52(2), pp.829-840, Feb. 2014.

[12] A. Saepuloh, N. Aisyah, M. Urai, "Detecting Surface Structures after Large Eruption of Mt. Merapi in 2010 Using ALOS/PALSAR Data," Procedia Earth and Planetary Science, Vol. 12, pp. 84-92, Dec. 2015.

[13] N. Demir, M. Kaynarcaa, S. Oya, "Extraction of Coastlines with Fuzzy Approach Using SENTINEL-1 SAR Image," ISPRS-International Archives of the Photogrammetry, Remote Sensing and Spatial Information Sciences, Vol.1, pp. 747-51, June 2016.

[14] Z. Liu, F. Li, N. Li, R. Wang, H. Zhang, "A Novel region-merging approach for coastline extraction from Sentinel-1A IW mode SAR imagery," IEEE Geoscience and Remote Sensing Letters, Vol. 13(3), pp. 324-328, Mar. 2016.

[15] A. Bhattacharya, A. Muhuri, S. De, S. Manickam, A. C. Frery, "Modifying the Yamaguchi four-component decomposition scattering powers using a stochastic distance," IEEE Journal of Selected Topics in Applied Earth Observations and Remote Sensing, Vol 8(7), pp. 3497-506, Jul. 2015 Jul.

[16] A. Moreira, P. Prats-Iraola, M. Younis, G. Krieger, I. Hajnsek and K. P. Papathanassiou, "A tutorial on synthetic aperture radar," IEEE Geoscience and Remote Sensing Magazine, Vol. 1, pp. 6-43, March 2013.

[17] B. Zou, Y. Zhang, N. Cao, N. P Minh, "A four-component decomposition model for PolSAR data using asymmetric scattering component," IEEE Journal of Selected Topics in Applied Earth Observations and Remote Sensing, Vol. 8(3), pp. 1051-1061, Mar. 2015.

[18] R. W. G. Carter, Coastal environments: an introduction to the physical, ecological, and cultural systems of coastlines. Academic Press, 3rd ed., Oct. 2013.

[19] T. A. Łabuz, "A review of field methods to survey coastal dunes—experience based on research from South Baltic coast," Journal of Coastal Conservation, Vol. 20(2), p.p 175-190, Apr. 2016.

[20] W. M. Jeong, H. Cho, W. Baek, "Analysis of the long-term wave characteristics off the coast of Daejin," Journal of Korean Society of Coastal and Ocean *Engineers*, Vol. 27(2), pp. 142-7, 2015.